

# Journal of Biomedical Optics

[SPIEDigitalLibrary.org/jbo](http://SPIEDigitalLibrary.org/jbo)

## **Optical micromanipulation of active cells with minimal perturbations: direct and indirect pushing**

Chenlu Wang  
Sagar Chowdhury  
Satyandra K. Gupta  
Wolfgang Losert

# Optical micromanipulation of active cells with minimal perturbations: direct and indirect pushing

Chenlu Wang,<sup>a,b</sup> Sagar Chowdhury,<sup>c</sup> Satyandra K. Gupta,<sup>c</sup> and Wolfgang Losert<sup>b,d</sup>

<sup>a</sup>University of Maryland, Biophysics Graduate Program, College Park, Maryland

<sup>b</sup>University of Maryland, Institute for Research in Electronics and Applied Physics, College Park, Maryland

<sup>c</sup>University of Maryland, Department of Mechanical Engineering, College Park, Maryland

<sup>d</sup>University of Maryland, Department of Physics, College Park, Maryland

**Abstract.** The challenge to wide application of optical tweezers in biological micromanipulation is the photodamage caused by high-intensity laser exposure to the manipulated living systems. While direct exposure to infrared lasers is less likely to kill cells, it can affect cell behavior and signaling. Pushing cells with optically trapped objects has been introduced as a less invasive alternative, but the technique includes some exposure of the biological object to parts of the optical tweezer beam. To keep the cells farther away from the laser, we introduce an indirect pushing-based technique for noninvasive manipulation of sensitive cells. We compare how cells respond to three manipulation approaches: direct manipulation, pushing, and indirect pushing. We find that indirect manipulation techniques lessen the impact of manipulation on cell behavior. Cell survival increases, as does the ability of cells to maintain shape and wiggle. Our experiments also demonstrate that indirect pushing allows cell–cell contacts to be formed in a controllable way, while retaining the ability of cells to change shape and move. © 2013 Society of Photo-Optical Instrumentation Engineers (SPIE) [DOI: 10.1117/1.JBO.18.4.045001]

Keywords: optical tweezers; photodamage; indirect pushing; *Dictyostelium discoideum*; cell viability; cell shape dynamics.

Paper 12789R received Dec. 12, 2012; revised manuscript received Feb. 19, 2013; accepted for publication Feb. 21, 2013; published online Apr. 1, 2013.

## 1 Introduction

Light beams exert small forces on objects, and for objects smaller than tens of micrometers, the forces can be designed to “grasp” a particle in an optical beam and move it to a desired position.<sup>1–4</sup> In recent years, a number of research groups found optical micromanipulation particularly useful for biological objects because of the ability of optical tweezers to precisely control the trapped object’s position, orientation, and speed.<sup>5–8</sup> Studies have been carried out on cells with a wide range of sizes: from bacteria, which are less than a micrometer, to red blood cells, which are usually less than 10 micrometers, to mammalian cells, which are tens of micrometers (T-cells).<sup>9–12</sup> Micromanipulation via optical trapping forces involves focusing a laser beam directly on cell samples.<sup>13–15</sup> Due to the extreme focusing of the laser in optical traps down to the diffraction limit, considerable photodamage can be inflicted on trapped cells, including the death of cells as noted by Ashkin, Dziedzic, and Yamane.<sup>5</sup> A range of assays has shown that focused laser light can also affect cell function without destroying the cell. Aside from heating, the photodamage mechanism has been proposed to be due to the creation of reactive oxygen through two-photon absorption.<sup>16–18</sup> These damages can affect the cells in various ways that become visible only in careful studies. For example, *Escherichia coli* is found to stop replicating after optical trapping.<sup>14</sup> Another investigation found that the internal pH of *E. coli* and *Listeria* bacteria declined because of direct trapping.<sup>19</sup> Even without direct exposure to the focused laser beam, yeast cells are found to divide less after optical trapping.<sup>20</sup>

Since photodamage causes a significant negative impact on cells, many in-depth studies have investigated various methods of maximizing cell health. First, it was found that 830 and 970-nm laser wavelengths were significantly less harmful to CHO cells and *E. coli* cells<sup>13,21</sup> than the nearby wavelength region from 870 to 910 nm. However, another group found only a weak dependence of *E. coli* viability on wavelengths in the range of 840 to 930 nm, with the total dose of laser light the dominant parameter determining the ability of cells to express genes.<sup>22</sup> Moreover, some studies indicate that the threshold at which light may lead to cell damage is very low compared to the laser power needed for optical micromanipulation. Using 1064 nm, Rasmussen, Oddershede, and Siegmund found that the internal pH (a measure of viability) of both *E. coli* and *Listeria* bacteria declined at laser intensities as low as 6 mW (i.e., 21.6 J for a 1-h exposure).<sup>19</sup> Ayano et al. showed that cell damage to *E. coli* was linearly dependent on the total dose received and found that cell division ability was affected at a dose larger than 0.35 J.<sup>23</sup> Furthermore, Aabo et al.’s study indicates that the photodamage to *Saccharomyces cerevisiae* depends on both the laser power and the accumulated dose.<sup>24</sup>

In the studies we mention above, photodamage can be minimized by minimizing light intensity or optimizing laser wavelength (but this also results in weakening the manipulation capabilities when directly manipulating cells), and choosing a laser wavelength that is optimal for the particular cell line and biological process (but which requires intensive calibration). In addition, preferred wavelengths are generally in the infrared, whereas visible lasers are generally less expensive, safer, and more common in labs and industry. Thus, we focus on using a pushing approach used previously and develop a new

Address all correspondence to: Wolfgang Losert, University of Maryland, Institute for Research in Electronics and Applied Physics, College Park, Maryland. Tel: 301-405-0629; Fax: 301-405-1678; E-mail: [wlosert@umd.edu](mailto:wlosert@umd.edu)

indirect pushing approach to minimize the exposure of the manipulated cell to any laser light, so the light intensity and wavelength of the trapping beam no longer noticeably affect cell viability. Direct pushing is a method by which we manipulate target cells by assistant objects that are directly trapped by laser beams. This minimizes the direct exposure of the target cells to the laser light. Microbeads, microrods, and some other micromaterials can be used to assist in the process.

The pushing approach to cell manipulation research has been carried out previously with assistance from microobjects, such as silica beads<sup>25</sup> and erythrocytes.<sup>26</sup> In these studies, the microobjects were attached to cells and applied forces to cells, and the resulting cell response was investigated. However, for other studies, it may be advantageous not to attach the object to the cells permanently. One reason to minimize contact between cells and pushing objects is that in cells with very active shapes (e.g., *Dictyostelium* cells<sup>27</sup> and human epithelial cells<sup>28</sup>), the shape dynamics and cell activity change upon adhesive contact with a surface. Hence, we prevent the pushing bead and cell from sticking to each other. In this investigation, this process is straightforward—both cells and beads are negatively charged and thus repel each other unless the charges are strongly screened by the buffer medium. Beads are removed from the cells after they have been manipulated.

We had previously developed a pushing technique that we called indirect optical gripping, in which we utilized holographic optical tweezers to hold six silica beads and form a small three-dimensional (3-D) trapping pocket.<sup>29</sup> In this procedure, a single cell can be placed in the trapping pocket and transported to the goal position.<sup>30,31</sup> The gripper, as well as some other optical manipulation methods that grip an object touching the cell, are less invasive to the target cell, as it reduces the light exposure during optical trapping. But it does not completely eliminate exposure of the target cell to the light cone,<sup>29</sup> and a fixed size or shape of target cells is required for applying these methods easily. However, many types of motile cells have very dynamic cell shapes and continuously generate protrusions and retractions on their membranes.<sup>27,32–34</sup> In this paper, we introduce a simple pushing approach, shown in Fig. 1(b), to manipulate cells indirectly, which not only reduces photodamage but also is suitable for manipulating cells with active shapes.

Our direct pushing method still exposes the pushed object to some laser light during the manipulation process. Thus, we also introduce indirect pushing, as shown in Fig. 1(c), where the laser beam does not overlap with cells. Note that in this indirect pushing, none of the trapped objects touches the cell, whereas in what is commonly called “indirect manipulation,” the trapped object usually touches the cell.<sup>26</sup>

Previous works estimated photodamage by observing different cell properties: growth and division of cells after optical trapping,<sup>14,24</sup> the rotation rate of the flagella in bacteria,<sup>13</sup> cloning efficiency of CHO cells,<sup>21</sup> viscoelastic properties,<sup>25</sup> or pH change in the cytosol.<sup>19</sup> Here, we introduce a new simple measure of cell viability: the ability of cells to wiggle and change shape. Unlike most previous works, which assessed viability from static properties, this measure is based on shape dynamics of the cell.

Dynamic shape and motility are significant properties to cells. It is widely believed that extending protrusions is necessary to many types of cells for migration, as cells use protrusions to adhere to surfaces and drag the cell body forward. Also, cells have different protrusion dynamics under different

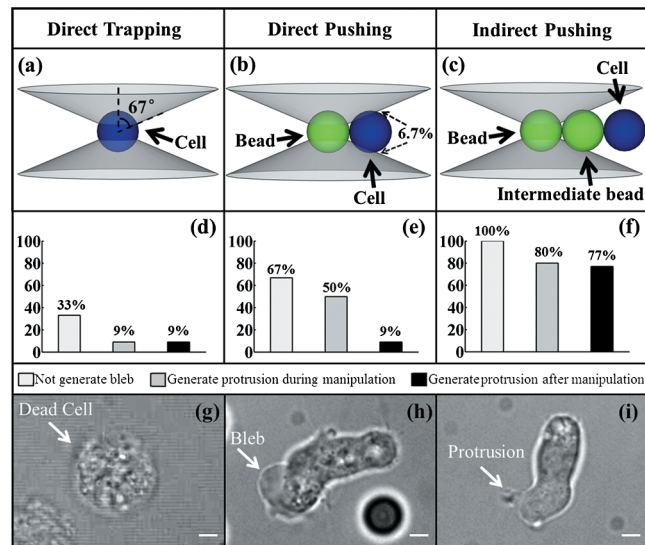


**Fig. 1** Viability test of *Dictyostelium* cells under different optical manipulation methods. (a)–(c) Schematic of manipulation methods. The diameter of the silica beads and cells is  $5\ \mu\text{m}$ . The angular aperture is  $67^\circ$  for the objective. (b): In equilibrium,  $6.7\%$  (in volume) of the target cell is exposed to the laser cone. (d)–(f) Tests indicating viability of cells with increasing sensitivity. Percentage of cells that do not generate blebs (often a precursor to cell death, light gray bars), generate protrusions during manipulation (dark gray bars) and still generate protrusions 5 min after manipulation (black bars). (g)–(i) representative figures of a dead cell, a blebbing cell, and a cell that is generating protrusions at its front. Scale bars in (g)–(i) are  $2\ \mu\text{m}$ .

circumstances.<sup>27</sup> Thus, protecting cells from damage to their shape dynamics is crucial when studying the motility and migration mechanism of the manipulated cells. Since the shape dynamics are driven by cytoskeletal dynamics, such as the polymerization and disassembly of actin filaments, changes of cell shape dynamics indicate that the active mechanical properties of the cell have changed.<sup>35</sup>

To study shape dynamics of manipulated cells, we use amoeboid cells of *Dictyostelium discoideum*. *Dictyostelium* cells have similar chemotaxis and migration mechanisms as some cancer cells; hence, their migration mechanism has been widely studied as a model system. When *Dictyostelium* migrates on a surface, cells elongate and periodically generate protrusions along the cell membrane. The protrusions usually start at the leading edge of the cell and then travel to the back on one side of the cell body, so they form a protrusion “wave” on the cell membrane. Often, adhesion to the surface strongly affects cell shape and protrusion dynamics. Thus, we focus on suspended cells that cannot adhere to the surface (see Sec. 2 for details). Suspended cells can be manipulated and moved with pN optical force, yet still exhibit protrusion waves after indirect pushing.

## 2 Materials and Methods

### 2.1 Optical Setup

Multiple optical point traps are generated by using a 532-nm green laser (Nd:YAG 5 W, Spectra-Physics, Newport Corporation, Irvine, California) coupled with a Nikon inverted light microscope and integrated with a Biorryx system (Arryx Inc., Chicago, Illinois). Though the 532-nm green laser is known to be harmful to cells, it presents a worst-case scenario that makes it easier to detect differences in photodamage with

different manipulation methods. Our indirect pushing method keeps cells viable even when hundreds of milliwatts of laser power at 532 nm are used for manipulation. A spatial light modulator has been built on this setup to customize the multitrap arrangement within 3-D spaces. With a Nikon 60X NA 1.4 oil immersion objective, the Biorix system can arrange up to 100 point traps within the operating region of about  $100 \times 100 \mu\text{m}^2$  and about  $10 \mu\text{m}$  above or below the focal plane. The same objective was used for both optical trapping and imaging. The cell manipulation process and long-term cell shape dynamics were imaged at 15 frames per second by a CCD camera (Foculus, Aegis Electronic Group, Gilbert, Arizona) and at 1 frame per second by a CCD camera (Ueye, IDS GmbH, Obersulm, Germany), respectively.

## 2.2 Preparations of *Dictyostelium* Cell, Human MCF-10A Mammary Epithelial Cells, and Silica Beads

*D. discoideum* lives as a single-cell amoeba when there is sufficient nutrition in the environment. Upon starvation, wild *Dictyostelium* is able to sense its neighboring cells and collectively migrate to an aggregation center, and eventually forms a slug, which helps the whole cell group move faster during the food searching. The wild *Dictyostelium* (AX3) cells were grown in an HL-5 medium at concentrations no higher than  $5 \cdot 10^6$  cells/mL at  $21^\circ\text{C}$ .<sup>36</sup> In these experiments, we starved and developed cells for five hours in a development buffer (DB: 5 mM  $\text{KH}_2\text{PO}_4$ ; 5 mM  $\text{Na}_2\text{HPO}_4 \cdot 7\text{H}_2\text{O}$ ; 2 mM  $\text{MgSO}_4$ ; 0.2 mM  $\text{CaCl}_2$ ) with pulses of 75 nM of cAMP every 6 min, as described in other papers.<sup>37,38</sup> Developed cells were harvested after 5 h by centrifuging 500  $\mu\text{L}$  of liquid from a develop flask at 9000 rpm for 3 min. The cell pellets were dissolved in 500  $\mu\text{L}$  of distilled water or phosphate buffer (PB: 5 mM  $\text{KH}_2\text{PO}_4$ ; 5 mM  $\text{Na}_2\text{HPO}_4 \cdot 7\text{H}_2\text{O}$ ).

The MCF-10A cells were grown in an incubator in which the humidified atmosphere was kept at  $37^\circ\text{C}$  and 5%  $\text{CO}_2$ , in the DMEM/F12 media with 5% horse serum, 10  $\mu\text{g}/\text{mL}$  insulin (Invitrogen), 10 ng/mL epidermal growth factor (EGF) (Peprotech, Rocky Hill, New Jersey), 0.5  $\mu\text{g}/\text{mL}$  hydrocortisone (Sigma, St. Louis, Missouri), and 100 ng/mL cholera toxin (Sigma, St. Louis, Missouri). For these experiments, cells were harvested from the culture flask by adding Trypsin (Invitrogen, Life Technologies, Carlsbad, California), and the supernatant were centrifuged at 350 rpm for 5 min. The cell pellet was dissolved in 6 mL growth media, and 10  $\mu\text{L}$  cells were added to a well of a  $\mu$ -slide eight-well chamber (Ibidi, Martinsried, Germany).

Silica beads (5  $\mu\text{m}$ ) are used as optical trapping assistants in indirect manipulation approaches. A microbead solution was prepared by mixing 2  $\mu\text{L}$  of an original silica microspheres solution (Bangs Laboratories, Fishers, Indiana) with 1 mL distilled water.

## 2.3 Suspended Cells and Beads

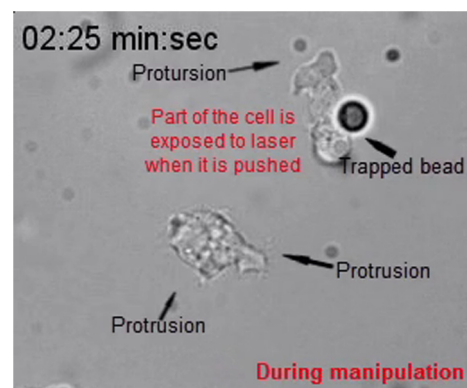
In order to have enough time to manipulate cells and beads, the electrostatic force is utilized in experiments with *Dictyostelium* cells to keep cells and beads from sticking to the glass surface. The surface of cover glass, *Dictyostelium* cells, and silica beads are all negatively charged, so they repel each other because of the Coulomb force when they get close together. After adding cells to a normal buffer, as in a standard experiment protocol,

cells gradually settle to the surface from suspension. Once placed on the surface, they adhere and start to spread; i.e., they form a growing contact area with the surface. The reason that they are able to overcome the repellent Coulomb force is that the cations in the buffer screen out the negative charge on cell membranes and surfaces.<sup>39</sup> In this study, we add cells and beads to distilled water so that the Coulomb force between cells and a glass surface can keep them suspended for manipulation. When studying cell-cell interaction, the lack of charge screening may also lead to repulsion between negatively charged cells. Thus, polyethyleneglycol (PEG) coated glass slides (from MicroSurface Inc., St. Louis, Missouri) are also used in the experiment shown in Sec. 3.3 to keep cells from adhering to the surface.

## 3 Results and Analysis

### 3.1 Viability of Cells After Optical Manipulation

We used three manipulation approaches on *Dictyostelium* cells: direct trapping, direct pushing, and indirect pushing. To show the configurations of different manipulation approaches and illustrate how the focus laser cones intersect with trapped beads or cells, we gave schematic figures of these three methods, as shown in Fig. 1(a)–1(c). The diameter of the silica beads is 5  $\mu\text{m}$ . The cells are assumed to be spherical, with similar size to the silica beads. The angular aperture (the angle between the cone and the direction of the laser beam) is  $67^\circ$  for the objective (comparable to other high NA objectives needed for optical trapping) used in this study. Unlike direct trapping [Fig. 1(a); see Video 1 for a representative direct trapping process], where the laser beam directly focuses on the target cell, the direct pushing approach [Fig. 1(b)] limits a cell's exposure to light (see Video 2 for a representative direct pushing process). As shown in Fig. 1(b), in equilibrium, with the trapped bead at the focal point of the laser, 6.7% (in volume) of the target cell is exposed to the laser cone. However, this is the lower limit of the volume exposed to laser light. If cells are larger than beads (5  $\mu\text{m}$  in diameter) or can deform their shape, the exposed volume can be higher. For example, *Dictyostelium* cells and epithelial cells are typically over 15  $\mu\text{m}$  in diameter, and the *Dictyostelium* cells actively deform their shapes. Using a bigger bead (at least 8  $\mu\text{m}$  in diameter in this example case) could possibly keep the cell out of the laser cone, but bigger beads cannot be stably trapped against its gravitational force with our optical tweezer system. The third method, indirect pushing, is shown



**Video 1** Direct pushing on *Dictyostelium* cells (MOV, 3.0 MB) [URL: <http://dx.doi.org/10.1117/1.JBO.18.4.045001.1>].

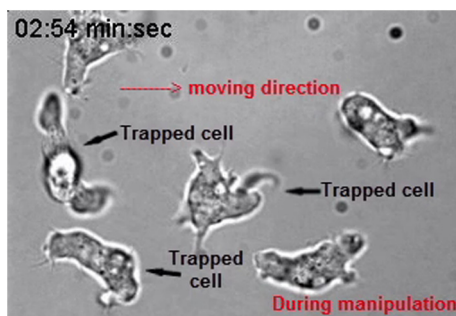




**Video 2** Indirect pushing on *Dictyostelium* cells (MOV, 10.5 MB) [URL: <http://dx.doi.org/10.1117/1.JBO.18.4.045001.2>].

in Fig. 1(c): The target cell is pushed by an intermediate bead, and the intermediate bead is pushed by another bead that is directly trapped by the laser beam. These two beads and the cell do not stick to each other (e.g., if the manipulation involves putting cells together into larger collections, beads have to be removed from the cell group). The directions of the forces that the directly trapped bead applies to the intermediate bead are tuned depending on the relative position of the intermediate bead and the target cell. How to push indirectly on the cells in a reliable manner has been described elsewhere.<sup>40</sup> When the target cell is pushed indirectly, the cell remains at least several microns away from the directly trapped bead and thus is not directly exposed to the light cone of the trapping laser (see Video 3 for a representative indirect pushing process).

Viability tests of these three manipulation methods were performed on a set of suspended *Dictyostelium* cells (21 cells for direct trapping, 18 cells for direct pushing, and 26 cells for indirect pushing). Videos 1–3 are representative videos that present the survival of unmanipulated cells with the manipulated cells in the same field of view. As shown in these videos, the cells were active before manipulation. To maintain constant conditions, the output laser power was set to 0.2 W, and the manipulation times remained between 40 and 50 s [i.e., (laser power) × (exposure time) = 8 to 10 J]. Four criteria were used here to estimate the photodamage [Fig. 1(d)–1(f)]: survival, the generation of blebs on the membrane, the generation of protrusions during manipulation, and the generation of protrusions after manipulation.



**Video 3** Direct trapping on *Dictyostelium* cells (MOV, 7.08 MB) [URL: <http://dx.doi.org/10.1117/1.JBO.18.4.045001.3>].

Note that the 532-nm green laser that we used is known to be harmful to cells. Thus, our study presents a worst-case scenario that makes it easier to detect differences in photodamage with different manipulation methods.

Dead *Dictyostelium* cells [shown in Fig. 1(g)] are easy to distinguish from living cells because they do not keep their membrane intact. All cells survived after all three manipulation approaches (data not shown). However, some living cells generate membrane blebs during manipulations, which usually indicates that cells cannot retain their cortical tension and are unhealthy.<sup>41–43</sup> A representative cell with a membrane bleb is shown in Fig. 1(h). As shown in Fig. 1(d)–1(f), the percentage of cells that generate blebs during trapping drops from 67% to 0% from a direct trapping approach to an indirect pushing approach.

*Dictyostelium* cells migrate, and they need to extend protrusions in order to move forward. When *Dictyostelium* cells migrate on a surface, they generate new protrusions every 20 s on average.<sup>27</sup> Thus, during the 45-second manipulation in this viability test, a healthy cell normally will be able to generate protrusions. But, as shown in Fig. 1(d)–1(f), only 9% of the cells under direct trapping extend protrusion during the manipulation, and this number increases to 50% and 80% when using the direct pushing and indirect pushing methods, which reveals that only indirect pushing approach does not have significant negative impact on cells in terms of generating protrusions in a short time of optical trapping.

Nevertheless, photodamage could have a long-term effect on cells. To study that, cells have been observed for at least 5 min after each manipulation. As shown in Fig. 1(d)–1(f), only after indirect pushing, most of the cells (77%) are found to be able to generate protrusions in 5 min after manipulation, while only 9% of the cells could generate protrusions after the other two types of manipulations. Thus, the indirect pushing approach shows no significant long-term photodamage on *Dictyostelium* cells.

### 3.2 Shape Analysis of Cells After Optical Manipulation

The viability test indicates that the indirect pushing method does not cause long-term photodamage in the generation of new protrusions, but the shape dynamics of the cell could be changed. As we learned from crawling *Dictyostelium* cells, protrusions should not only be generated, but also travel on cell membranes like a wave. Thus, a shape dynamics analysis method that we previously developed has been used to analyze shapes of cells after optical trapping (see details in Ref. 27).

The shapes of cells after direct or indirect pushing are analyzed as shown in Fig. 2. In Fig. 2(b), indirect pushing of a cell toward another cell is shown. In Fig. 2(a) and 2(b), *Dictyostelium* cells maintain a polarized, elongated shape. The polarized end that generates new protrusions is considered as the “front” (i.e., “head”) of the cell, and the other end is the “back” (i.e., “tail”) of the cell.

To analyze shape dynamics, 400 points on the cell boundary are extracted by an active contour algorithm.<sup>44</sup> The curvature along each point on the boundary is calculated and used as a metric for shape. Figure 2(c) shows an image of a representative cell with its extracted boundary, colored with curvature value. Two main high-curvature regions are seen (red indicates high-positive curvature): one in the front (black arrow), and the other in the back (white arrow). In addition, there are small high-curvature regions (small red regions, red arrows).

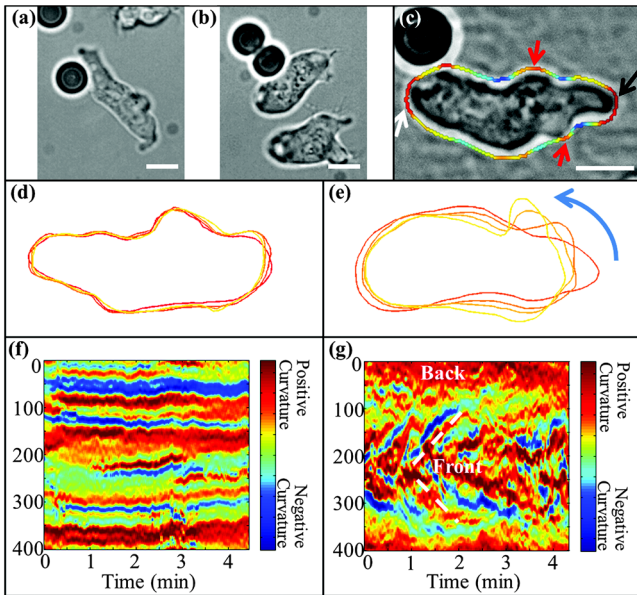


**Fig. 2** Shape analysis of *Dictyostelium* cells after optical manipulation. (a) A cell that is pushed directly by a silica bead. (b) A cell that is pushed indirectly by a silica bead through an intermediate bead. (c) Extracted outlines of a representative polarized cell (red: positive curvature; blue: negative curvature). (d) Overlaid shapes of a cell manipulated by direct pushing (20 s apart; red: initial shape). (e) Overlaid shapes of a cell manipulated by indirect pushing (2 s apart; red: initial shape). (f) Curvature versus time plot of a cell manipulated by direct pushing. (g) Curvature versus time plot of a cell manipulated by indirect pushing. Scale bars in (a)–(c) are 5  $\mu\text{m}$ .

To visualize shape dynamics, we overlay cell shape outlines from different points in time. Figure 2(d) shows overlaid cell shapes after direct pushing [the cell is the same as in Fig. 2(a)]. As we can see, although the cell retains its polarity and looks similar to a healthy cell [shown in Fig. 2(c)], its overall shape does not change notably in 80 s, indicating that the cell's active shape changes after direct pushing. After indirect pushing, however [the cell in the Fig. 2(b)], cells continue to change shape [Fig. 2(e)]. Cell shape dynamics do not seem to be affected by indirect pushing. Localized protrusions travel from the front to the back of the cell (blue arrow), consistent with our prior observations.

To visualize and quantify shape dynamics over minutes, we plot a kymograph (space-time plot) where color indicates local curvature (red: positive curvature; blue: negative curvature; curvature value shows in the color bar). Each vertical line in the kymograph represents one shape outline at a different time, for a total of 4.5 min [Fig. 2(f) and 2(g)]. After direct pushing, the shape of the cell remains unchanged with time: The front and back, as well as additional small protrusions form multiple straight red lines in Fig. 2(f). After indirect pushing [Fig. 2(g)], tilted red lines are visible that start at the front of the cell, indicating protrusions that travel as a wave from the front of the cell to the back (white dotted lines), similar to what we reported previously on healthy *Dictyostelium* cells.<sup>34</sup>

### 3.3 Indirect Pushing Allows for Studies of Cell–Cell Adhesion

Next, we demonstrate an example of how indirect pushing may be used to address a biological question: namely, how cell–cell contact affects cell behavior. Often, cell–cell contact is studied

when cells are anchored to a surface, and therefore, cell–cell contact competes with cell–surface contact. However, many cells can be brought into suspension or be prevented from anchoring to the surface, at least temporarily. In that case, they also lack the ability to push off the surface and move, and thus they need to be manipulated in order to get in contact with other cells in a controlled way.

We first investigated cell–cell adhesion in cells suspended in distilled water. Unlike mammalian cells, the amoeboid cells we investigate (*Dictyostelium*) have special organelle that allow them to survive in distilled water. As shown in Video 3, when two cells were pushed together, we find that they did not form stable cell–cell adhesion. Instead, after indirect pushing stopped, they moved apart immediately, though cells were viable by our strictest standards. They maintained their shape dynamics until they moved out of the field of view 19 min after manipulation.

To assess whether this lack of cell–cell adhesion was related to the absence of a buffer medium that screens charges and limits repulsive forces between cells, we used cells in a buffer, but on PEG-coated glass slides to prevent cell–surface adhesion. We find that cells in buffer are able to stick to others when they are pushed into contact. This process is shown in Fig. 3. In Fig. 3(a) and 3(b), two suspended cells are generating new protrusions (black arrows) before manipulation. A bead (white arrow) is directly trapped by an optical trap and moved toward an intermediate bead and cell A. The indirect pushing process is shown in Fig. 3(b)–3(d) as these two cells are arranged along their polarization direction (head to tail) and are pushed together to form direct cell–cell contact. This manipulation process lasts

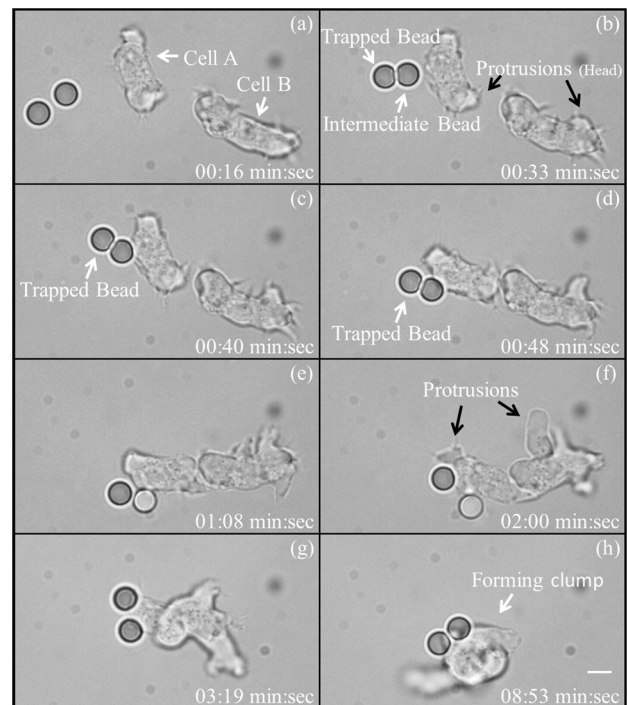


**Fig. 3** Indirect pushing of two *Dictyostelium* cells allows testing of cell–cell adhesion with controlled cell polarity. (a) and (b) A bead is directly trapped by the optical trap and moved toward another bead and cell A. (c) and (d) Cell A is pushed indirectly by the trapped bead through the intermediate bead. (e) The manipulation stops after 1 min, and the two *Dictyostelium* cells are able to stick together. (f)–(h) The two adhered *Dictyostelium* cells extend protrusions and form a clump in the following 8 min. Scale bar: 5  $\mu\text{m}$ .



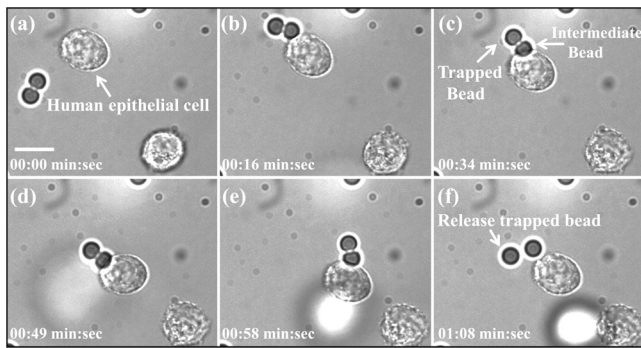


**Fig. 4** Indirect pushing of an MCF-10A cell. (a) A bead is directly trapped directly by the optical trap and pushed to another bead, and moves toward an MCF-10A cell. (b)–(e) Cell is pushed indirectly from a different direction by the trapped bead through the intermediate bead. (f) After manipulation, the trapped bead is released from trapping. Scale bar in (a) is 10  $\mu\text{m}$ .

for about 40 s. After the manipulation stops, these two cells still extend protrusions (black arrows) and retain dynamic shapes. The cells remain in contact and eventually form a clump several minutes after manipulation, as shown in Fig. 3(h). We have carried out this procedure successfully eight times, demonstrating that it is possible to generate cell–cell contact with controlled polarity for biophysical investigations.

### 3.4 Manipulating Epithelial Cells via Indirect Pushing

The indirect pushing method introduced in this paper is useful for nonadherent cells. But it also can be used on adherent cells, taking advantage of the slow process of cell–substrate adhesion. Mammalian cells usually adhere to surfaces or an extracellular matrix, and utilize cell–surface adhesion to migrate. When adhered to a surface, these cells cannot be manipulated with optical tweezers since adhesion forces are in the nN range, which is stronger than optical forces. However, there can be a delay of up to half an hour between the time that cells settle to the surface and the time that they start to adhere, as reported in Ref. 45, among others. The delay time can be adjusted by varying the surface coating concentration. For example, we studied MCF-10A human breast cells (see Fig. 4). After placement in an eight-well chamber (Ibidi), it was possible to push cells indirectly with silica beads before the cells stick on the surface for more than 30 min.

## 4 Conclusions and Future Work

This study presents evidence that indirect pushing significantly reduces the potential photodamage to target cells. By indirect pushing, we mean optical trapping of beads, which push another bead, which in turn pushes on a cell. Unlike direct manipulation or direct pushing (where cells are pushed directly by beads and parts of cells are still exposed to the trapping beam), indirect pushing does not expose cells to laser light. Indeed, cells remain viable even when hundreds of milliwatts of laser power at 532 nm (i.e., in a harmful wavelength range) are used for manipulation. Our study focused on the worst-case scenario (manipulation with laser light of a wavelength that is known to harm cells) to demonstrate that the indirect pushing method is broadly applicable to a wide range of laser wavelengths.

In the viability study, most of the indirectly pushed cells are able to maintain their polarized shapes during manipulation.

More important, most cells maintained their shape dynamics after manipulation. Thus, indirect pushing may be applied to study many interesting biological questions regarding cell motility or mechanical properties of pairs or groups of cells, the small building blocks of tissues and organs.

One of the challenges of manual indirect pushing is that the intermediate bead could slip out from the configuration. Thus, it requires constant tuning of the pushing direction. However, by integrating robotic planning techniques, it is not a challenge to reliably execute indirect pushing operations. The robotic control is achieved through a feedback loop that takes the current states of the trapped bead, intermediate bead, and the target cell into account to produce optimal action to move the trap so that the cell can be transported toward the desired goal location. The instability of the intermediate bead due to random Brownian motion does not affect the stability of the controller. The authors were even successful in manipulating smaller cells; e.g., yeast cells that have a smaller contact area between intermediate bead and cell, which makes the pushing more challenging.<sup>40</sup> In addition, we have developed an approach that is able to trap multiple beads automatically at the same time and move them on different trajectories using holographic tweezers, which will allow us to push multiple cells indirectly to different positions to form collective cell patterns in a controlled way.<sup>30,46–48</sup>

### Acknowledgments

We thank Rachel Lee (Losert Lab, UMD) and Dr. Carole Parent (NCI, NIH) for providing MCF-10A cells. This research has been supported by NSF Grants CMMI-0835572 and CPS-0931508.

### References

1. A. Ashkin et al., "Observation of a single-beam gradient force optical trap for dielectric particles," *Opt. Lett.* **11**(5), 288–290 (1986).
2. A. Ashkin, "Forces of a single-beam gradient laser trap on a dielectric sphere in the ray optics regime," *Biophys. J.* **61**(2), 569–582 (1992).
3. D. G. Grier, "A revolution in optical manipulation," *Nat. Photon.* **424**(6950), 810–816 (2003).
4. G. C. Spalding, J. Courtial, and R. Di Leonardo, "Holographic optical tweezers," Chapter 6, in *Structured Light and Its Applications: An Introduction to Phase-Structured Beams and Nanoscale Optical Forces*, pp. 139–168, Academic Press, Waltham, Massachusetts (2008).
5. A. Ashkin, J. M. Dziedzic, and T. Yamane, "Optical trapping and manipulation of single cells using infrared laser beams," *Nature* **330**(6150), 769–771 (1987).
6. A. Ashkin and J. Dziedzic, "Optical trapping and manipulation of viruses and bacteria," *Science* **235**(4795), 1517–1520 (1987).
7. S. Kulin et al., "Real-time measurement of spontaneous antigen–antibody dissociation," *Biophys. J.* **83**(4), 1965–1973 (2002).
8. A. G. Banerjee et al., "Survey on indirect optical manipulation of cells, nucleic acids, and motor proteins," *J. Biomed. Opt.* **16**(5), 051302 (2011).
9. H. Zhang and K.-K. Liu, "Optical tweezers for single cells," *J. R. Soc. Interf.* **5**(24), 671–690 (2008).
10. C. T. Lim et al., "Experimental techniques for single cell and single molecule biomechanics," *Mater. Sci. Eng. C* **26**(8), 1278–1288 (2006).
11. Y. Tan et al., "Mechanical characterization of human red blood cells under different osmotic conditions by robotic manipulation with optical tweezers," *IEEE Trans. Biomed. Eng.* **57**(7), 1816–1825 (2010).
12. X. Wang et al., "Enhanced cell sorting and manipulation with combined optical tweezer and microfluidic chip technologies," *Lab Chip* **11**(21), 3656–3662 (2011).
13. K. C. Neuman et al., "Characterization of photodamage to *Escherichia coli* in optical traps," *Biophys. J.* **77**(5), 2856–2863 (1999).
14. M. Ericsson et al., "Sorting out bacterial viability with optical tweezers," *J. Bacteriol.* **182**(19), 5551–5555 (2000).

15. J. M. Nascimento et al., "Analysis of sperm motility using optical tweezers," *J. Biomed. Opt.* **11**(4), 044001 (2006).
16. M. W. Berns, "A possible two-photon effect *in vitro* using a focused laser beam," *Biophys. J.* **16**(8), 973–977 (1976).
17. K. König et al., "Cell damage in near-infrared multimode optical traps as a result of multiphoton absorption," *Opt. Lett.* **21**(14), 1090–1092 (1996).
18. K. Svoboda and S. M. Block, "Biological applications of optical forces," *Annu. Rev. Biophys. Biomol. Struct.* **23**(1), 247–285 (1994).
19. M. B. Rasmussen, L. B. Oddershede, and H. Siegmundfeldt, "Optical tweezers cause physiological damage to *Escherichia coli* and *Listeria bacteria*," *Appl. Environ. Microbiol.* **74**(8), 2441–2446 (2008).
20. N. Arneborg et al., "Interactive optical trapping shows that confinement is a determinant of growth in a mixed yeast culture," *FEMS Microbiol. Lett.* **245**(1), 155–159 (2005).
21. H. Liang et al., "Wavelength dependence of cell cloning efficiency after optical trapping," *Biophys. J.* **70**(3), 1529–1533 (1996).
22. U. Mirsaidov et al., "Optimal optical trap for bacterial viability," *Phys. Rev. E* **78**(2), 021910 (2008).
23. S. Ayano et al., "Quantitative measurement of damage caused by 1064-nm wavelength optical trapping of *Escherichia coli* cells using on-chip single cell cultivation system," *Biochem. Biophys. Res. Commun.* **350**(3), 678–684 (2006).
24. T. Aabo et al., "Effect of long- and short-term exposure to laser light at 1070 nm on growth of *Saccharomyces cerevisiae*," *J. Biomed. Opt.* **15**(4), 041505 (2010).
25. M. Dao, C. T. Lim, and S. Suresh, "Mechanics of the human red blood cell deformed by optical tweezers," *J. Mech. Phys. Solids* **51**(11–12), 2259–2280 (2003).
26. P. Grigaravičius, K. O. Greulich, and S. Monajembashi, "Laser microbeams and optical tweezers in ageing research," *ChemPhysChem* **10**(1), 79–85 (2009).
27. M. K. Driscoll et al., "Cell shape dynamics: from waves to migration," *PLoS Comput. Biol.* **8**(3), e1002392 (2012).
28. G. F. Weber, M. A. Bjerke, and D. W. DeSimone, "A mechano-responsive cadherin-keratin complex directs polarized protrusive behavior and collective cell migration," *Develop. Cell* **22**(1), 104–115 (2012).
29. B. Koss et al., "Indirect optical gripping with triplet traps," *J. Opt. Soc. Am. B* **28**(5), 982–985 (2011).
30. S. Chowdhury et al., "Gripper synthesis for indirect manipulation of cells using holographic optical tweezers," *IEEE Intl. Conf. Intell. Robots Automat.*, 2749–2754, IEEE, Saint Paul, Minnesota (2012).
31. S. Chowdhury et al., "Automated manipulation of biological cells using gripper formations controlled by optical tweezers," in *IEEE Trans. Automat. Sci. Eng.* (Conditionally accepted for publication) (2013).
32. P. Friedl, S. Borgmann, and E.-B. Bröcker, "Amoeboid leukocyte crawling through extracellular matrix: lessons from the *Dictyostelium* paradigm of cell movement," *J. Leuk. Biol.* **70**(4), 491–509 (2001).
33. N. P. Barry and M. S. Bretscher, "Dictyostelium amoebae and neutrophils can swim," *Proc. Natl. Acad. Sci. U. S. A.* **107**(25), 11376–11380 (2010).
34. M. K. Driscoll, J. T. Fourkas, and W. Losert, "Local and global measures of shape dynamics," *Phys. Biol.* **8**(5), 1–9 (2011).
35. G. Gerisch et al., "Mobile actin clusters and traveling waves in cells recovering from actin depolymerization," *Biophys. J.* **87**(5), 3493–3503 (2004).
36. M. Sussman, Chapter 2, "Cultivation and synchronous morphogenesis of *Dictyostelium* under controlled experimental conditions," in *Methods in Cell Biology*, A. S. James, Ed., pp. 9–29, Academic Press, Waltham, Massachusetts (1987).
37. P. Devreotes et al., Chapter 17, "Transmembrane signaling in *Dictyostelium*," in *Methods in Cell Biology*, A. S. James, Ed., pp. 299–331, Academic Press, Waltham, Massachusetts (1987).
38. C. P. McCann et al., "Cell speed, persistence, and information transmission during signal relay and collective migration," *J. Cell Sci.* **123**(10), 1724–1731 (2010).
39. M. Socol et al., "Synchronization of *Dictyostelium discoideum* adhesion and spreading using electrostatic forces," *Bioelectrochemistry* **79**(2), 198–210 (2010).
40. A. Thakur et al., "Automated indirect micromanipulation of biological cells using indirect pushing to minimize photo-damage," in *6th Intl. Conf. Micro- and Nanosystems (MNS)*, Chicago, Illinois (2012).
41. L. W. Janson and D. L. Taylor, "In vitro models of tail contraction and cytoplasmic streaming in amoeboid cells," *J. Cell Biol.* **123**(2), 345–356 (1993).
42. J. C. Mills et al., "Apoptotic membrane blebbing is regulated by myosin light chain phosphorylation," *J. Cell Biol.* **140**(3), 627–636 (1998).
43. G. Gerisch et al., "Chemoattractant-controlled accumulation of coronin at the leading edge of *Dictyostelium* cells monitored using a green fluorescent protein–coronin fusion protein," *Curr. Biol.* **5**(11), 1280–1285 (1995).
44. X. Chenyang and J. L. Prince, "Snakes, shapes, and gradient vector flow," *IEEE Trans. Image Proc.* **7**(3), 359–369 (1998).
45. B. J. Dubin-Thaler et al., "Nanometer analysis of cell spreading on matrix-coated surfaces reveals two distinct cell states and STEPs," *Biophys. J.* **86**(3), 1794–1806 (2004).
46. S. Chowdhury et al., "Automated indirect transport of biological cells using planar gripper formations," in *8th IEEE Intl. Conf. Automat. Sci. Eng.*, Seoul, Korea, pp. 267–272 (2012).
47. S. Chowdhury et al., "Automated cell transport in optical tweezers assisted microfluidic chambers," *IEEE Trans. Automat. Sci. Eng.* **PP**(99), 1–10 (2012).
48. A. G. Banerjee et al., "Realtime path planning for coordinated transport of multiple particles using optical tweezers," *IEEE Trans. Automat. Sci. Eng.* **9**(4), 669–678 (2012).